Validation of Cogswell's Convergent Flow Analysis

PASCALE REVENU,* JACQUES GUILLET, CHRISTIAN CARROT, and ALAIN ARSAC

Laboratoire de Rhéologie des Matières Plastiques, Faculté de Sciences et Techniques, Université Jean Monnet, 23, Rue du Docteur Paul Michelon, 42023 Saint-Etienne Cedex 2, France

SYNOPSIS

The behavior of two polymers, namely, low-density and linear low-density polyethylenes, was studied in transient and steady-state shear and elongational flows. The predictions of Wagner's model with a damping function using a generalized invariant were calculated. The model appears to be suitable for predictions of the shear and elongational transient flows on the range of strains experimentally tested. The shear flow curves can also be recovered by the model on a very broad range of shear rates. The model is then used to assess extensional data obtained with the convergent flow analysis proposed by Cogswell.

INTRODUCTION

The determination of the elongational flow behavior of molten polymers is still an open problem. It remains difficult to reach very large strains and strain rates with the existing elongational rheometers. That is why indirect methods of determination of the elongational viscosity have been proposed, such as convergent flow analysis. For the last two decades, data obtained by different direct methods and/or data obtained with indirect methods have been frequently compared, but contradictions still exist and the problem of determining the elongational viscosity is therefore not totally solved.

On the other hand, the development of softwares for flow simulation in processing tools brings rheologists along to look for a constitutive equation able to predict the rheological behavior of molten polymers especially in mixed-flow situations. Even if that has not come to an end yet, the literature shows numerous examples of models and of comparisons between predictions and experimental data, as far as it is possible to get some. For instance, the integral Wagner model[1] has been widely used in transient and steady-state shear flows and in transient elongational flows. It was usually shown to be relatively suitable to predict experimental data. In this study, we proposed to use this model to validate the indirect method of determination of elongational flow curves proposed by Cogswell,[2] often tested and discussed.

BACKGROUND AND THEORY

Indirect Method of Determination of the Elongational Viscosity

The indirect method of determination of the elongational viscosity which is the most widely used, because it can deal with the largest variety of fluids, is isothermal melt spinning. In a previous article,[3] it was shown that this transient elongational flow is similar to the flow encountered in elongational viscosimeters. The viscosity obtained by such a method, which is a function of both the strain rate and the time, cannot be considered as a steady viscosity and elongational flow curves cannot be determined. In fact, the range of strain rates and strains reached, drastically limited by the influence of extrudate swell, draw resonance, or filament breaking, is too narrow.

Cogswell[2] developed an analytical analysis to determine the "elongational viscosity" from capillary rheometer data. He considered that the pressure drop at the entry of the die is due to shear and elongational contributions.

* To whom correspondence should be addressed.

Journal of Applied Polymer Science, Vol. 62, 1783–1792 (1996)
 CCC 0021-8995/96/111783-10

If θ is the half-angle of convergence, a simple trigonometric argument yields that the pressure drop due to simple shear flow is

$$\Delta P_S = A\eta/\tan\theta \tag{1}$$

where η is the viscosity under simple shear at the shear rate at the wall of the converging part and A is a proportionality factor. By a similar argument, the pressure drop due to extensional flow is

$$\Delta P_E = B\eta_E \tan\theta \tag{2}$$

where η_E is the elongational viscosity, and B, a proportionality factor.

The two contributions are supposed to be separable and simply additive; therefore,

$$\Delta P = \Delta P_S + \Delta P_E \tag{3}$$

In practice, the flow pattern is such that it varies along the distance from the die entry plane. For unrestricted convergence from a reservoir to a die, it is assumed that the flow will adopt a streamline that involves the least pressure drop:

$$\frac{d\Delta P_E}{d\tan\theta} = 0 \tag{4}$$

Assuming that the viscosity under simple shear can be described by a power-law relationship over a limited stress range and that the elongational viscosity is independent of stress, he solved these equations for an infinite set of very short tapes and obtained analytical expressions for the elongational viscosity and stress:

$$\eta_E = \frac{9(n+1)^2}{32\eta}\left(\frac{\Delta P_0}{\dot\gamma_a}\right)^2 \tag{5}$$

$$\tau_E = \tfrac{3}{8}\Delta P_0(n+1) \tag{6}$$

where $\dot\gamma_a$ is the apparent shear rate; ΔP_0, the entrance pressure drop; and n, the flow index.

This method provides data at significantly higher strain rates (100 s^{-1}) than do the previous ones. However, because of the numerous assumptions of the theory and of some surprising results in the literature, the method has been widely discussed and some contradictions still remain. For instance, in 1969, Cogswell[4] compared results obtained from a steady-state experiment with a melt tensile rheometer and from convergent flow analysis (CFA). For both a poly(methyl methacrylate) and a linear low-density polyethylene (LDPE), he found a really good agreement. In 1977, Shroff et al.[5] found a good coincidence between a set of data from isothermal melt-spinning and a set of data calculated by CFA for a polystyrene, a polypropylene, and a high-density polyethylene. Nevertheless, they finally stipulated that the agreement could be fortuitous. In 1989, Laun and Schuch[6] compared the elongational viscosities from isothermal homogeneous drawing in different elongational viscosimeters and those calculated from the Cogswell analysis. Even if in some cases they found a good agreement, they concluded that no general rule could be given. For several polymers, Covas and Carneiro[7] found considerable differences between the calculated viscosities and those determined with a Rutherford extensional rheometer, but they concluded that the qualitative rheological behavior in elongation can be correctly assessed by CFA.

Although the assumptions made by Cogswell in his theory might be questionable, inconsistencies between the authors can also find their origin in unreliable experimental values of elongational viscosity. For example, the experimental values obtained from isothermal fiber-spinning are questionable, the elongational rates are not constant along the threadline, and the steady state is seldom achieved. On the other hand, with an elongational viscosimeter, the values are much more reliable but, unfortunately, the level of strain rates reached is much smaller than the one obtained with convergent flows and the results are not easily comparable. As a consequence, our aim was to identify the numerical parameters of a suitable constitutive equation using a well-controlled flow situation and then to compare the prediction of this equation in a steady elongational flow with experimental results obtained from CFA.

The Model

One of the models which has been widely used and which was shown to be relatively suitable to predict experimental data is Wagner's model.[1] Derived from Lodge's rubberlike liquid theory,[8] Wagner's model is based on a concept of separability. It assumes that the memory function is the product of a time-dependent function and of a strain-dependent function. The constitutive equation therefore takes the following form in the case of an increasing deformation:

$$\underset{\approx}{\tau}(t) = \int_{-\infty}^{t} m(t-t')h(I_1, I_2)\underset{\approx}{C}_t^{-1}(t')\,dt' \tag{7}$$

where $m(t - t')$ is the memory function; $h(I_1, I_2)$, the damping function; and $\underset{\approx}{C}_t^{-1}$, the Finger relative strain tensor.

In the case of a discrete Maxwellian relaxation spectrum, the memory function is related to the linear relaxation modulus by

$$m(t) = \sum_{i=1} \frac{\eta_i}{\lambda_i^2} \exp\left(-\frac{t}{\lambda_i}\right) = -\frac{dG(t)}{dt} \tag{8}$$

where λ_i are the relaxation times of the discrete relaxation spectrum; $\eta_i = g_i \cdot \lambda_i$, the viscosity contributions corresponding to the different λ_i and g_i, the modulus contributions.

Different forms have been proposed for the damping function, but only a few of them are suitable in shear and in elongation. The form which has been chosen in this work is the sigmoidal form, first proposed in shear by Soskey and Winter[9]:

$$h(I_1, I_2) = \frac{1}{1 + a(I - 3)^{b/2}} \tag{9}$$

where I is Wagner's general invariant,[10] defined as

$$I = \beta I_1 + (1 - \beta) I_2 \tag{10}$$

with

$$I_1 = I_2 = \gamma^2 + 3 \qquad \text{in shear} \tag{11}$$

$$I_1 = e^{2\varepsilon} + 2e^{-\varepsilon} \quad I_2 = (e^{-2\varepsilon} + 2e^{\varepsilon}) \qquad \text{in elongation} \tag{12}$$

The damping function has to be calculated in the appropriate flow situation, which means that we need to determine one function in shear and one in elongation. They can be determined experimentally by a derivation from the tangential and elongational stresses, respectively, in transient experiments as proposed by Wagner[11] in elongation and by Fulchiron et al.[12] in shear:

$$h(\gamma) = \frac{\dfrac{\sigma(\gamma)}{G(\gamma)} - \dfrac{1}{\dot{\gamma}} \displaystyle\int_0^{\gamma} \sigma(\gamma') \frac{m(\gamma')}{G^2(\gamma')} \cdot d\gamma'}{\gamma} \qquad \gamma = \dot{\gamma} t \tag{13}$$

$$h(\varepsilon) = \frac{\dfrac{\sigma(\varepsilon)}{G(\varepsilon)} - \dfrac{1}{\dot{\varepsilon}} \displaystyle\int_0^{\varepsilon} \sigma(\varepsilon') \frac{m(\varepsilon')}{G^2(\varepsilon')} \cdot d\varepsilon'}{e^{2\varepsilon} - e^{-\varepsilon}} \qquad \varepsilon = \dot{\varepsilon} t \tag{14}$$

Once the memory function and the damping functions are known, the different rheological functions can be calculated as followed:

Transient shear viscosity in stress growth:

$$\eta^+(t, \dot{\gamma}) = \int_0^t m(s) h(\dot{\gamma} s) s \, ds + G(t) h(\dot{\gamma} t) t \tag{15}$$

Transient first normal shear stresses coefficient in stress growth:

$$\Psi_1^+(t, \dot{\gamma}) = \int_0^t m(s) h(\dot{\gamma} s) s^2 \, ds + G(t) h(\dot{\gamma} t) t^2 \tag{16}$$

Transient elongational viscosity in stress growth:

$$\eta_E^+(t, \dot{\varepsilon}) = \frac{1}{\dot{\varepsilon}} \int_0^t m(s) h(\dot{\varepsilon} s) [e^{2\dot{\varepsilon} s} - e^{-\dot{\varepsilon} s}] \, ds + \frac{1}{\dot{\varepsilon}} h(\dot{\varepsilon} t) [e^{2\dot{\varepsilon} t} - e^{-\dot{\varepsilon} t}] G(t) \tag{17}$$

Steady shear viscosity:

$$\eta(\dot{\gamma}) = \int_0^{\infty} m(s) h(\dot{\gamma} s) s \, ds \tag{18}$$

First normal stresses coefficient:

$$\Psi_1(\dot{\gamma}) = \int_0^t m(s) h(\dot{\gamma} s) s^2 \, ds \tag{19}$$

Steady elongational viscosity:

$$\eta_E(\dot{\varepsilon}) = \frac{1}{\dot{\varepsilon}} \int_0^t m(s) h(\dot{\varepsilon} s) [e^{2\dot{\varepsilon} s} - e^{-\dot{\varepsilon} s}] \, ds \tag{20}$$

Wagner's model has been extensively tested in shear and transient elongational flows. It has been shown to give rather good predictions of nonlinear behavior.[1,11,12] It is one of the most widely used models in elongation because it predicts the existence of a steady-state regime for large strains.

EXPERIMENTAL

Materials

Two commercial polyethylenes were selected for this study: a low-density polyethylene (LDPE) and a linear low-density polyethylene (LLDPE), different mainly in the degree and the nature of their branching. Their molecular and physical characteristics are summarized in Table I.

Table I Molecular and Physical Characteristics of the Polymers

Material	$\overline{M_n}$ (g/mol)	$\overline{M_w}$ (g/mol)	$\overline{M_w}/\overline{M_n}$	MFI	Density at 20°C (g/cm^3)	Density at 160°C (g/cm^3)
LLDPE	19,100	120,000	6.3	0.73	0.922	0.76
LDPE	26,700	120,000	4.5	0.8	0.921	0.75

Techniques

Shearing tests have been accomplished in three geometries: (i) parallel plates, (ii) capillary rheometer, and (iii) cone and plate:

- Dynamic measurement of storage and loss moduli G' and G'' were carried out using a Rheometrics dynamic analyzer, Model 700 (RDA), in the dynamic mode with the parallel 25 mm-diameter plate geometry. Tests were performed between 140 and 200°C for frequencies ranging between 0.01 and 500 rad/s. Above 190°C, tests were carried out under a dry nitrogen atmosphere, using 40 mm-diameter plates, to avoid thermooxidative degradation.
- A Rheometrics mechanical spectrometer, Model 800 (RMS), was used with a 25 mm-diameter plate and a 0.1 rad angle cone geometry to perform both stress growth and steady-state experiments at 160°C.
- An Instron capillary rheometer (Model 3211 equipped with a 0–2000 kg load cell) was used at 140, 160, and 190°C. Three series of dies, each characterized by a constant diameter (0.75, 1.25, 2 mm), with a length-to-diameter ratio ranging from 1 to 12.5 were used. Experiments at constant plunger speeds ranging from 0.06 to 20 cm/min, imposing a constant apparent wall shear rate, were performed whenever it was possible. In some cases, measurements were limited by the onset of melt fracture.

Elongational data were obtained from two different tests: (i) constant strain elongational rheometer and (ii) Cogswell convergent flow analysis:

- Transient tests were conducted on the elongational viscosimeter developed by Muller and Froelich[13] in which the sample is vertically and symmetrically stretched by two clamps, driven at an exponential velocity. The force-measuring device, clamps, and sample were immersed in a silicon-oil bath regulated at 160°C, with an oil density very close to that of the molten polyethylene. The samples were injection-molded and then annealed to avoid any residual stress in the material.
- The "steady-state" elongational viscosity data were obtained from the capillary rheometer data described above and eq. (5).

RESULTS AND DISCUSSION

Dynamic Tests

First, the time–temperature superposition was applied to the storage and loss moduli vs. the frequency curves, $G'(\omega)$ and $G''(\omega)$, to extend the frequency window at the reference temperature (160°C). The discrete relaxation times spectra at 160°C were then calculated using a nonlinear minimization procedure described by Carrot et al.[14] which lets the number of relaxation modes and the time values of these modes freely adjust. The two spectra obtained are shown in Table II, and using these values in a Maxwell model, the G' and G'' curves can be recovered within a 3% error in the explored frequency window. But the procedure fails to recover the longest and the shortest relaxation times of the spectrum. If the zero shear viscosity as calculated agrees with the value determined by a Cole–Cole representation, the calculated equilibrium modulus G_N^0 (Table III) is quite different from the data given in the literature, due to an obvious lack of experimental data at high frequencies.

Transient Flows

Knowing the discrete relaxation spectrum and stress growth data, the experimental damping functions were obtained using eqs. (13) and (14). In Figures 1 and 2, the experimental damping functions obtained for shear rates ranging from 0.2 and 2 s^{-1} are presented. In this range of shear rates, the separability assumption is verified, as long as the data obtained at different strain rates can be superposed.

The damping function in elongation is presented for elongational rates ranging from 0.2 to 2 s^{-1}. In the short time range, because of the starting delay time of the rheometer and because uncertainties in

Table II Relaxation Spectrum of LLDPE and LDPE at 160°C

LLDPE		LDPE	
λ_i (s)	η_i (Pa·s)	λ_i (s)	η_i (Pa·s)
$1.28 \cdot 10^{-4}$	$2.367 \cdot 10^{2}$	$6.45 \cdot 10^{-4}$	$9.810 \cdot 10^{1}$
$6.12 \cdot 10^{-3}$	$1.346 \cdot 10^{3}$	$5.35 \cdot 10^{-3}$	$2.855 \cdot 10^{2}$
$4.10 \cdot 10^{-2}$	$3.363 \cdot 10^{3}$	$2.85 \cdot 10^{-2}$	$7.679 \cdot 10^{2}$
$2.77 \cdot 10^{-1}$	$4.691 \cdot 10^{3}$	$1.55 \cdot 10^{-1}$	$2.619 \cdot 10^{3}$
$2.01 \cdot 10^{0}$	$3.726 \cdot 10^{3}$	$8.91 \cdot 10^{-1}$	$6.464 \cdot 10^{3}$
$1.57 \cdot 10^{1}$	$2.007 \cdot 10^{3}$	$4.58 \cdot 10^{0}$	$1.219 \cdot 10^{4}$
$1.35 \cdot 10^{2}$	$9.563 \cdot 10^{2}$	$2.34 \cdot 10^{1}$	$1.325 \cdot 10^{4}$
		$1.18 \cdot 10^{2}$	$7.296 \cdot 10^{3}$

the experimental data are important, eq. (14), involving both a difference and a numerical integration, leads to physically unrealistic values of the damping functions. On the other hand, the maximum Hencky strain is attainable with the elongational rheometer hardly reaching 3. Consequently, the damping function can be known only on a narrow range of strains. From these experimental data, the adjustable parameters (a, b, and β) of eq. (9) were calculated (Table IV).

a and b were obtained from shear tests. Then, with the memory function and an analytical expression of the damping function in shear being known, the predictions of the model in transient flow can be calculated with eqs. (15) and (16). The calculations of the damping function, stress, and first normal stresses coefficient growth are compared to the experimental data in Figures 1–6.

Keeping a and b constant, β was evaluated from the elongational data. It should be noted that, especially for the LLDPE, for which strain hardening is not very pronounced, the determination of this last parameter is not easy. That is why the parameter was chosen from the best fit of both experimental damping function and stress growth experiments. In spite of uncertainties of the parameters, it can be seen in Figures 1 and 2 that the analytical forms chosen give a rather good fit of the experimental data. Moreover, the values of β are consistent with those mentioned by Papanastasiou et al.[15] The predictions of the model in elongation are calculated with eq. (17) and compared to the experimental data in Figures 7 and 8.

In the range of experimental shear rates, both the transient behavior and the values of the tangential and normal stresses at the plateau are well recovered. In elongation, the stress growth is recovered for elongational strain rates up to 2.6 s^{-1}. It can therefore be concluded that Wagner's model is well predictive of the different transient flows.

Steady-state Shear Flows

With the cone and plate geometry, steady-state experiments were carried out. Viscosity (η) and first normal stresses differences (N1) were measured vs. shear rate. To reach high shear rates, capillary rheometry experiments were performed. All stress data were corrected using die entrance pressure drops determined from Bagley's diagrams. The plot of corrected stress obtained with the whole series of dies yields a unique curve, confirming the validity of the correction, whatever the temperature is. The Rabinowisch correction was applied. The power law index n was calculated from the local slope of a second-order polynome, fitting stress vs. shear rate on a double logarithmic scale. The shift factors are found to be identical to those from dynamical tests.

In Figures 9 and 10, different data are plotted. The equivalence between dynamic and steady-

Table III Viscoelastic Parameters at 160°C Determined (1) from Cole–Cole Representation and (2) from the Relaxation Spectra

Material	T (°C)	η_0 (1) (Pa·s)	η_0 (2) (Pa·s)	G_N^0 (2) (Pa)
LLDPE	160	$1.54 \cdot 10^{4}$	$1.44 \cdot 10^{4}$	$2.3 \cdot 10^{6}$
LDPE	160	$4.26 \cdot 10^{4}$	$4.30 \cdot 10^{4}$	$2.6 \cdot 10^{5}$

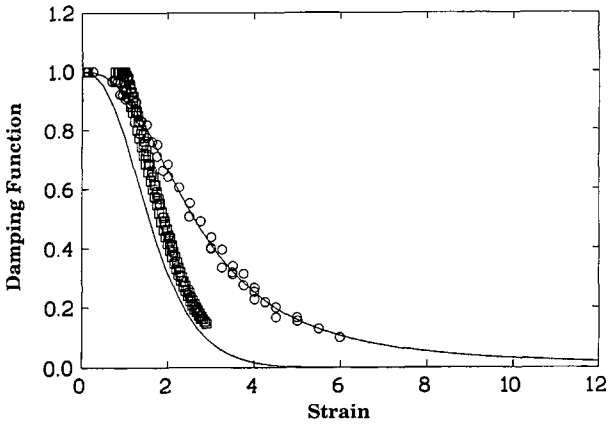

Figure 1 Damping functions of LLDPE at 160°C (○) in shear and (□) in elongation. (—) Fit according to eq. (9) with invariant (10).

state shear data can be observed only for LLDPE [$\eta(\dot{\gamma}) = |\eta^*(\omega)|_{(\omega=\dot{\gamma})}$]. For LDPE (Fig. 10), the quantities measured by capillary and cone and plate rheometers appear to be higher than the dynamic ones especially in the medium shear rate range [$\eta(\dot{\gamma}) > |\eta^*(\omega)|_{(\omega=\dot{\gamma})}$].

Wagner's model allows predictions of the steady-state rheological shear functions from eqs. (18) and (19). In Figures 9 and 10, calculated and experimental data of the viscosity and first normal stresses coefficient are shown to be in a very good agreement. For the LDPE for which the Cox–Merz rule does not apply, the calculated viscosities coincide with the steady-state viscosities obtained in steady-state shearing. If as shown by different authors[16,17] that the damping function might also depend on the strain history of the material, it is normal to have better agreement with the steady-state shearing data, since the same geometry was used and the strain was uniformly increasing during the tests. Wagner's model, using the damping function defined by Soskey and Winter,[9] predicts well the steady-state shear behavior.

Steady-state Elongational Flows

In the steady-state elongational mode, the predictions of Wagner's model are given by eq. (20). The "experimental elongational parameters" can be calculated from eqs. (5) and (6) using the capillary rheometer data presented above. Although Cogswell's theory has been established for 180° die entry angles, the data obtained in the capillary rheometer with 90° die entry angles were used. In fact, our measurements and Seriai's ones[18] showed that the die entry angle between 90° and 180° has no influence on the entrance pressure drops.

In his original study, Cogswell considered a power-law equation for the viscosity, which means that the power law index n is assumed to be constant whatever the shear rate is. As regards the shear flow curves, n obviously changes with $\dot{\gamma}$. The power law index has therefore been taken as a variable in the calculations ($n = A + B \log \dot{\gamma}$) of $\dot{\varepsilon}$ and η_E. The elongational flow curves of the LLDPE and of the LDPE are presented in Figures 11 and 12.

In spite of careful experiments of the shear flow parameters (temperature control along the reservoir, residence time in the reservoir at the beginning of the experiment), data are rather scattered. The parameter which seems to be at the origin of the discrepancy is the entrance pressure drop. A statistical approach done on the Bagley's regression shows that the error on the entrance pressure drops can reach 30% for the lowest shear rate tested, but otherwise ranges between 5 and 10%. This error is at least recovered on the elongational strain rate and is multiplied by two on the elongational rate.

Because Bagley's diagrams have often been discussed by authors such as Han[19] or Laun and Schuch,[6] we tried to confirm the validity of our data. As observed by Utracki and Schlund[20] on different polyethylenes, the plot on a double logarithmic scale of die entry pressure drops vs. apparent shear rate or vs. shear stress, for a contraction ratio ranging from 4.76 to 12.7 and whatever the die diameter is, gives an unique curve for each polymer (Fig. 13). In addition, the time–temperature superposition can successfully be applied using the shift factors obtained in linear viscoelasticity.

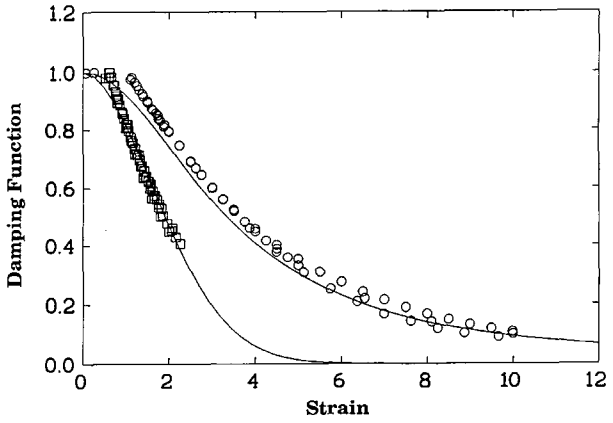

Figure 2 Damping functions of LDPE at 160°C (○) in shear and (□) in elongation. (—) Fit according to eq. (9) with invariant (10).

Table IV Values of the Adjustable Parameters of the Damping Functions

Functions	LDPE	LLDPE
$h(\gamma) = \dfrac{1}{1 + a\gamma^b}$	$a = 0.084$	$a = 0.086$
	$b = 2.06$	$b = 2.56$
$h(\varepsilon) = \dfrac{1}{1 + a[\beta(e^{2\varepsilon} + 2e^{-\varepsilon}) + (1 - \beta)(e^{-2\varepsilon} + 2e^{\varepsilon}) - 3]^{b/2}}$	$a = 0.084$	$a = 0.086$
	$\beta = 0.019$	$\beta = 0.02$
	$b = 2.06$	$b = 2.56$

The evolution of the entrance pressure drop can be well represented by a second-order polynome. Using these fitted entrance pressure drops, the elongational parameters were recalculated. Scattering is thus canceled, and for the two samples, these curves nicely smooth the scattered points (Figs. 11 and 12).

On the LLDPE flow curve (Fig. 11), two values of steady-state elongational viscosity data obtained with an elongational viscosimeter are presented. They are in good agreement with the previous data. Both the elongational rates at which the strain hardening appears and the ratio of the maximum viscosity to the Troutonian viscosity lie in the same order of magnitude as does the data found by Covas and Carneiro[7] and Laun and Schuch[6] by the same method on polyethylene with very similar molecular structures. Finally, as previously shown by Laun and Schuch,[6] it is seen that in elongation the thermodependence is of the same sort as in the shear: An Arrhenius-type rule gives a good evaluation of the viscosity at different temperatures in the explored range.

The comparison of the model predictions and of the data obtained from the CFA analysis is finally made in Figures 9 and 10. The occurrence of strain hardening, as well as the strain rate position (along the X-axis) of the maximum of viscosity calculated by the CFA are close to the data predicted by the model. The main disagreement lies in the value of the maximum viscosity on the LLDPE and in the viscosities at high strain rates for the LDPE.

The inaccuracies of the linear relaxation modulus and of the damping functions, due to a lack of data in dynamic tests or in transient stress growth, obviously do not lead to a significant divergence of the predictions in transient and steady-state shear flows and are therefore probably not at the origin of the differences in the steady-state elongational flow. They probably find their origin first in the level of viscosity which is quite low in the case of the LLDPE and which can lead to some degree of inaccuracy of the experimental data and, second, in the problem of residence time in the convergent. With time being an important parameter for elongational flows, the residence time in the convergent was compared to

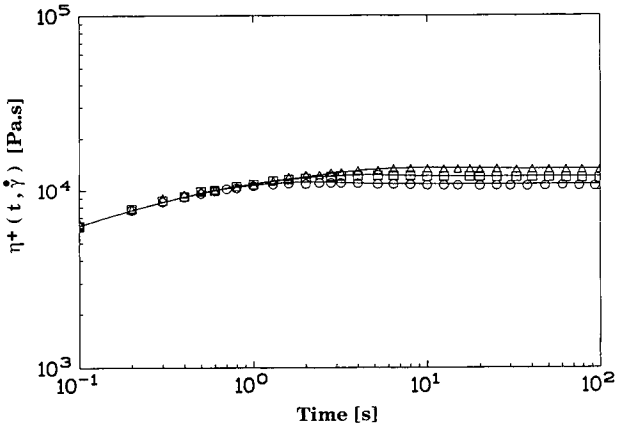

Figure 3 Transient shear viscosity of LLDPE at 160°C. (△) Experimental: 0.2 s^{-1}; (□) 0.5 s^{-1}; (○) 1 s^{-1}. (—) Calculated.

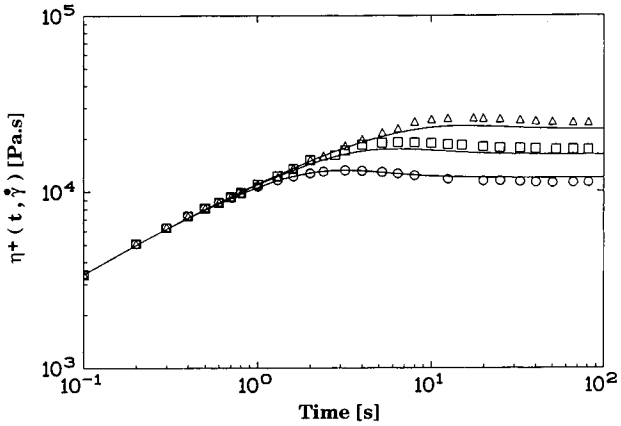

Figure 4 Transient shear viscosity of LDPE at 160°C. Experimental: (△) 0.2 s^{-1}; (□) 0.5 s^{-1}; (○) 1 s^{-1}. (—) Calculated.

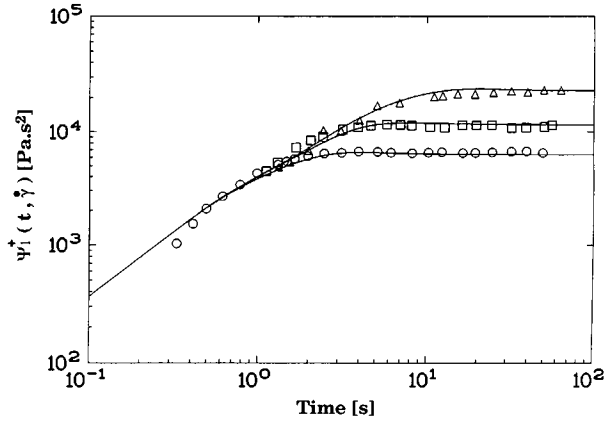

Figure 5 Transient first normal stresses difference coefficient of LLDPE at 160°C. Experimental: (△) 0.2 s^{-1}; (□) 0.5 s^{-1}; (○) 1 s^{-1}. (—) Calculated.

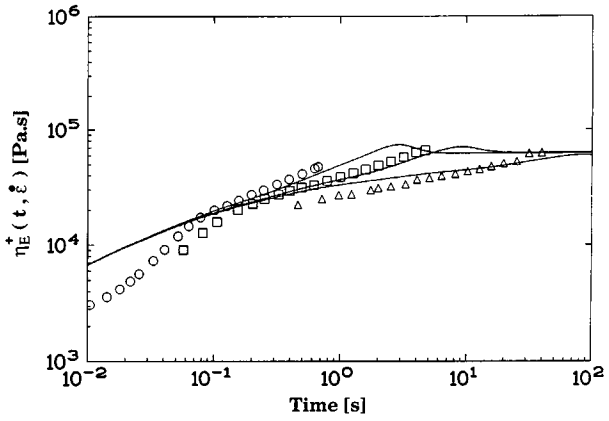

Figure 7 Transient elongational viscosity of LLDPE at 160°C. Experimental: (△) 0.2 s^{-1}; (□) 0.5 s^{-1}; (○) 1 s^{-1}. (—) Calculated.

the time required to obtain a stationary value of the viscosity, according to Wagner's model predictions. If at low shear rates the residence time is long enough, at high shear rates, this might be sometimes questionable. In the case of LLDPE, for instance, at elongational rates greater than 17 s^{-1}, the residence time was found to fall in the order of the maximum relaxation time of the spectrum.

CONCLUSION

The behavior of two polymers was studied in different flow situations. In shear and in elongation, the LLDPE and the LDPE, with equivalent molecular weight and close molecular weight distribution (according to GPC measurements), display very different flow behavior.

The influence on the linear viscoelastic behavior has been observed. The relaxation time corresponding to the maximum viscosity in the spectrum is 100 times higher in the case of the LDPE than of the LLDPE. Because of a long chain, the relaxation of the junctions is slower, shifting the spectrum to the long relaxation times. Newtonian and Troutonian viscosities appear at very low strain rates and are very high.

Nonlinear viscoelastic flow behavior is also strongly influenced. The decrease of the damping function is smoother in the case of LDPE. Long side branches might hinder complete retraction of the polymer chains and lead to a persistance of the junctions. The shear thinning appears at low strain rates and is much more pronounced. In elongation, strain hardening is more important and the maximum of viscosity is reached for lower strain rates than for LLDPE. Long-chain branching has a pre-

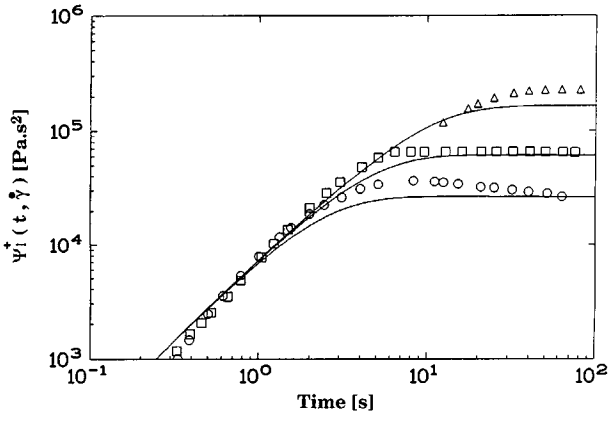

Figure 6 Transient first normal stresses difference coefficient of LDPE at 160°C. Experimental: (△) 0.2 s^{-1}; (□) 0.5 s^{-1}; (○) 1 s^{-1}. (—) Calculated.

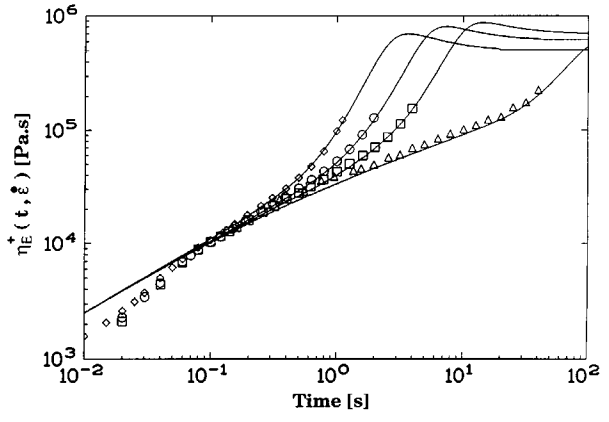

Figure 8 Transient elongational viscosity of LDPE at 160°C. Experimental: (△) 0.2 s^{-1}; (□) 0.5 s^{-1}; (○) 1 s^{-1}; (◇) 2 s^{-1}. (—) Calculated.

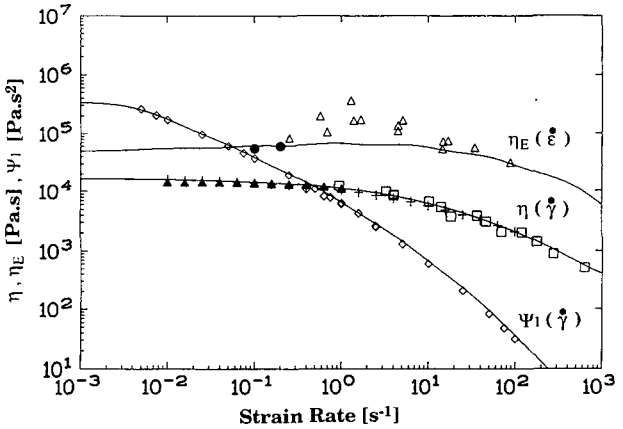

Figure 9 Steady-state functions for LLDPE at 160°C. Experimental: (△) elongational viscosity from CFA; (●) elongational rheometer. (◇) First normal stresses difference coefficient. Steady-state and dynamic shear viscosity determined with (▲) cone and plate geometry, (□) capillary rheometer, and (+) oscillatory parallel plates. (—) Calculated.

dominant effect (compared to the MWD) on the flow behavior in shear and in uniaxial elongation.

The predictions of Wagner's model with a damping function using a generalized invariant were calculated and compared to the experimental data. On the tested range of shear rates, the model gives very good predictions of the transient flows in shear and in uniaxial elongation. In shear, where the experimental data are very accurate, the steady-state flow behavior is recovered by the model. If the essence

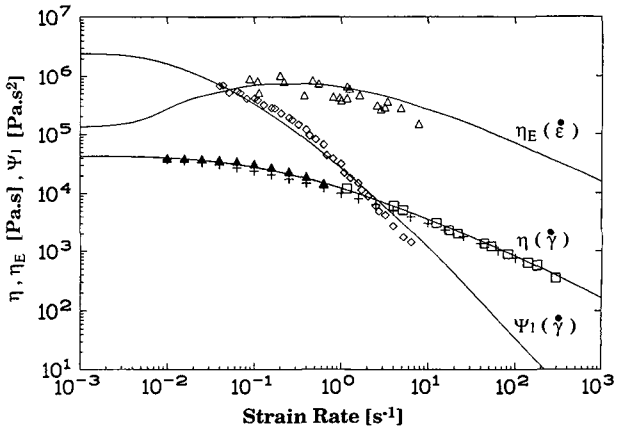

Figure 10 Steady-state functions for LDPE at 160°C (experimental and calculated). Experimental: (△) elongational viscosity from CFA. (◇) First normal stresses difference coefficient. Steady-state and dynamic shear viscosity determined with (▲) cone and plate geometry, (□) capillary rheometer, and (+) oscillatory parallel plates. (—) Calculated.

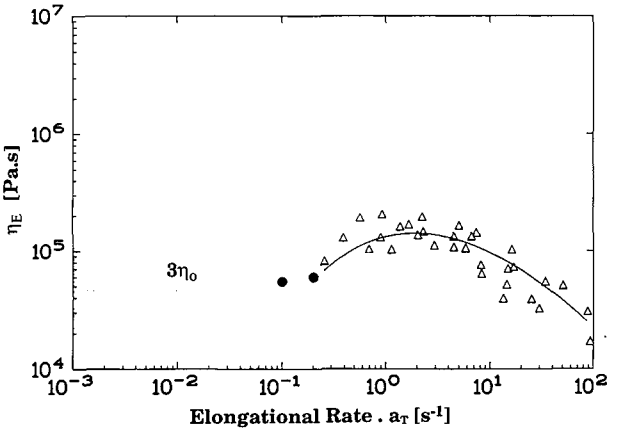

Figure 11 Master curve of elongational viscosity vs. strain rate at 160°C for LLDPE according to (△) Cogswell analysis, (—) using fitted entrance pressure drops, and (●) data from elongational viscosimeter.

of the model is accepted, the different functions used can be considered to be satisfying.

The convergent flow analysis proposed by Cogswell was used to determine the steady-state elongational viscosity of the two polyethylenes. The problem of the determination of the entrance pressure drops was shown to be determinant in this sort of analysis. Nevertheless, the data obtained are in rather good agreement with the predictions of Wagner's model. The divergences observed were related to the problems of residence time. In conclusion, the consistency of the numerous elongational data obtained by different techniques and the confrontation with data calculated by a pertinent Wagner model show that Cogswell's CFA is a good approach of the elongational flows at high strain rates.

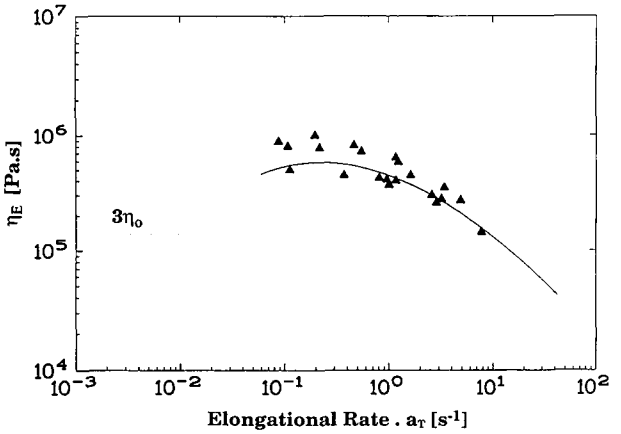

Figure 12 Master curve of elongational viscosity vs. strain rate at 160°C for LDPE according to (▲) Cogswell analysis, and (—) using fitted entrance pressure drops.

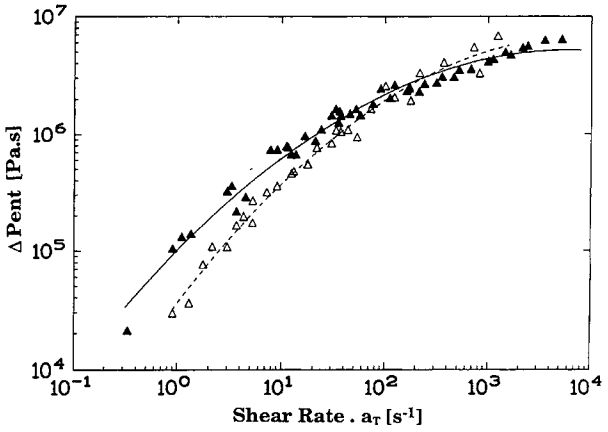

Figure 13 Master curve of die entry pressure drops vs. shear rate at 160°C. Experimental data (△) for LLDPE and (▲) for LDPE. (—) Polynomial fitting.

REFERENCES

1. M. H. Wagner, *Rheol. Acta,* **15,** 136 (1976).
2. F. N. Cogswell, *Polym. Eng. Sci.,* **12,** 64 (1972).
3. P. Revenu, J. Guillet, and C. Carrot, *J. Rheol.,* **37,** 1041 (1992).
4. F. N. Cogswell, *Rheol. Acta,* **8,** 187 (1969).
5. R. N. Shroff, L. V. Cancio, and M. Shida, *Trans. Soc. Rheol.,* **21,** 429 (1977).
6. H. M. Laun and H. Schuch, *J. Rheol.,* **33,** 119 (1989).
7. J. A. Covas and O. S. Carneiro, *Polym. Test.,* **9,** 181 (1990).
8. A. S. Lodge, *Rheol. Acta,* **7,** 379 (1968).
9. P. R. Soskey and H. H. Winter, *J. Rheol.,* **28,** 625 (1984).
10. M. H. Wagner, *Rheol. Acta,* **18,** 681 (1979).
11. M. H. Wagner, *J. Non-Newt. Fluid Mech.,* **4,** 39 (1978).
12. R. Fulchiron, V. Verney, and G. Marin, *J. Non Newt. Fluid Mech.,* **48,** 49 (1993).
13. R. Muller and D. Froelich, *Polymer,* **26,** 1477 (1985).
14. C. Carrot, J. Guillet, J. F. May, and J. P. Puaux, *Makromol. Chem. Theory Simul.* **1,** 215 (1992).
15. A. C. Papanastasiou, L. E. Scriven, and C. W. Macosko, *J. Rheol.,* **27,** 387 (1983).
16. H. M. Laun, *Rheol. Acta,* **17,** 1–15 (1978).
17. P. Revenu, PhD Thesis, Saint-Etienne, France, 1992.
18. M. Seriai, PhD Thesis, Saint-Etienne, France, 1991.
19. C. D. Han, *Rheology in Polymer Processing,* Academic Press, New York, 1976.
20. L. A. Utracki and B. Schlund, *Polym. Eng. Sci.,* **27,** 367 (1987).

Received May 1, 1996
Accepted May 20, 1996